

AD-A181 417

OPTICAL DATA PROCESSING(U) CARNEGIE-MELLON UNIV  
PITTSBURGH PA DEPT OF ELECTRICAL AND COMPUTER  
ENGINEERING D CASASANT JAN 86 AFOSR-TR-87-0482

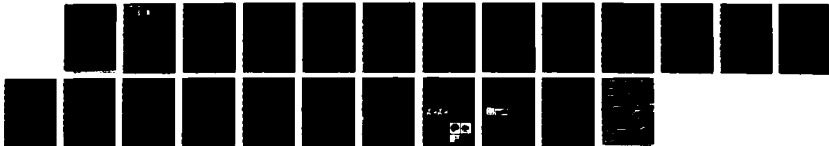
1/1

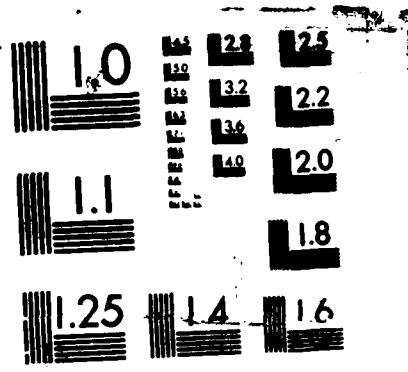
UNCLASSIFIED

AFOSR-84-0293

F/G 12/9

NL





MICROCOPY RESOLUTION TEST CHART  
NATIONAL BUREAU OF STANDARDS-1963-A

## REPORT DOCUMENTATION PAGE

1a. REPORT SECURITY CLASSIFICATION <b>Unclassified</b>		1b. RESTRICTIVE MARKINGS	
2a. SECURITY CLASSIFICATION AUTHORITY <b>DTIC SELECTED</b>		3. DISTRIBUTION / AVAILABILITY OF REPORT <b>Unlimited</b>	
2b. DECLASSIFICATION / DOWNGRADING SCHEDULE <b>JUN 1 8 1987</b>		5. MONITORING ORGANIZATION REPORT NUMBER(S) <b>AFOSR-TR- 87-0482</b>	
4. PERFORMING ORGANIZATION REPORT NUMBER(S) <b>AF-ODP-86</b>		5. MONITORING ORGANIZATION REPORT NUMBER(S) <b>AFOSR-TR- 87-0482</b>	
6a. NAME OF PERFORMING ORGANIZATION <b>Carnegie Mellon University</b>	6b. OFFICE SYMBOL (if applicable)	7a. NAME OF MONITORING ORGANIZATION <b>AFOSR/NE</b>	
6c. ADDRESS (City, State, and ZIP Code) <b>Department of Electrical and Computer Engg. Pittsburgh, PA 15213</b>		7b. ADDRESS (City, State, and ZIP Code) <b>Same as 8c</b>	
8a. NAME OF FUNDING / SPONSORING ORGANIZATION <b>AFOSR/NE</b>	8b. OFFICE SYMBOL (if applicable)	9. PROCUREMENT INSTRUMENT IDENTIFICATION NUMBER <b>AFOsr-84-0293</b>	
8c. ADDRESS (City, State, and ZIP Code) <b>ATTN: Lee Giles Bolling Air Force Base Washington, D.C. 20332</b>		10. SOURCE OF FUNDING NUMBERS	WORK UNIT ACCESSION NO.
		PROGRAM ELEMENT NO. <b>61102F</b>	PROJECT NO. <b>2305</b>
		TASK NO. <b>B1</b>	
11. TITLE (Include Security Classification) <b>Optical Data Processing</b>			
12. PERSONAL AUTHOR(S) <b>David Casasent</b>			
13a. TYPE OF REPORT <b>Interim Annual</b>	13b. TIME COVERED <b>FROM 1/86 TO 12/86</b>	14. DATE OF REPORT (Year, Month, Day) <b>January 1986</b>	15. PAGE COUNT <b>(3) + 156</b>
16. SUPPLEMENTARY NOTATION			
17. COSATI CODES		18. SUBJECT TERMS (Continue on reverse if necessary and identify by block number)	
FIELD	GROUP	Optical data processing, pattern recognition, feature extraction, moments, Hartley transforms, relational graphs, distortion-invariant filters, discriminant functions. <i>57</i>	
19. ABSTRACT (Continue on reverse if necessary and identify by block number)			
<p>Our research concerns optical data processing for missile guidance and target recognition. It uses pattern recognition techniques with an increasing use of knowledge base, inference machine and associative processor techniques. Our Year 2 work addresses devices (the liquid crystal television), Kalman filters, intrinsic features, iconic filters, and symbolic processors. These all represent quite novel optical processing concepts. Our work also concerns new architectures and concepts such as: relational graph processors, optical linear discriminant processors, model-based optical processors, hierarchical symbolic optical correlators, and optical associative processors.</p>			
20. DISTRIBUTION / AVAILABILITY OF ABSTRACT <input checked="" type="checkbox"/> UNCLASSIFIED/UNLIMITED <input type="checkbox"/> SAME AS RPT. <input type="checkbox"/> DTIC USERS		21. ABSTRACT SECURITY CLASSIFICATION <b>Unclassified</b>	
22a. NAME OF RESPONSIBLE INDIVIDUAL <b>David Casasent DR C Lee Giles</b>		22b. TELEPHONE (Include Area Code) <b>(412) 268-2464 767-4931</b>	22c. OFFICE SYMBOL <b>NE</b>

Block 18: Continued

symbolic correlators, optimal distortion invariant filters, intrinsic filters, iconic filters, relational graphs, optical linear discriminant functions, model-based processors, associative processors, symbolic hierarchical correlators.

g. h. i.

**AFOSR-TB- 87 - 0482**

# OPTICAL DATA PROCESSING

**Interim Report: Year 2  
January 1, 1986 - December 31, 1986  
Grant AFOSR-84-0293**

**Approved for public release;  
distribution unlimited.**

**SUBMITTED TO:**

**Air Force Office of Scientific Research  
Bolling Air Force Base  
Washington, D.C. 20332**

**ATTN: Dr. C. Lee Giles, AFOSR/NE**

**PREPARED BY:**

**Carnegie-Mellon University  
Department of Electrical and Computer Engineering  
Pittsburgh, PA 15213  
David Casasent, Principal Investigator  
Telephone: (412) 268-2464**

**AIR FORCE OFFICE OF SCIENTIFIC RESEARCH (AFOSR)  
NOTICE OF TRANSMISSION TO DTIC  
This technical report has been reviewed and is  
approved for public release under AFR 190-12.  
Distribution is unlimited.  
MATTHEW J. SPER  
Chief, Technical Information Division**

Accession For	
NTIS CRA&I	<input checked="" type="checkbox"/>
DTIC TAB	<input type="checkbox"/>
Unannounced	<input type="checkbox"/>
Justification	
By	
Distribution/	
Availability Codes	
Dist	Availability Special
A-1	



# Table of Contents

<b>ABSTRACT AND SUMMARY</b>	<b>1</b>
<b>1. INTRODUCTION</b>	<b>2</b>
<b>2. SUMMARY AND OVERVIEW</b>	<b>4</b>
2.1 SPATIAL LIGHT MODULATORS (SLMs) (Chapter 3, Liquid Crystal Television Correction)	4
2.2 FACTORIZED KALMAN FILTER (KF) ALGORITHM (Chapter 4)	4
2.3 FEATURE EXTRACTION (MOMENTS, FOURIER TRANSFORMS AND HARTLEY TRANSFORMS) (Chapters 5 and 6)	5
2.4 APPROACHES TO LARGE-CLASS ANALYSIS PROBLEMS (Chapters 7 and 12)	6
2.5 NEW ICONIC FILTERS FOR HIERARCHICAL PROCESSORS (Chapter 8-10)	8
2.6 COMPUTER GENERATED HOLOGRAM (CGH) FILTER SYNTHESIS (Chapter 11)	9
2.7 OPTICAL ARTIFICIAL INTELLIGENCE (Chapters 13-17)	9
<b>CHAPTER 2 REFERENCES</b>	<b>11</b>
<b>3. PHASE CORRECTION OF LIGHT MODULATORS</b>	<b>16</b>
<b>4. FACTORIZED EXTENDED KALMAN FILTER FOR OPTICAL PROCESSING</b>	<b>24</b>
<b>5. CALCULATION OF GEOMETRIC MOMENTS USING FOURIER PLANE INTENSITIES</b>	<b>36</b>
<b>6. GEOMETRIC MOMENTS COMPUTED FROM THE HARTLEY TRANSFORM</b>	<b>43</b>
<b>7. SIGNAL-TO-NOISE RATIO CONSIDERATIONS IN MODIFIED MATCHED SPATIAL FILTERS</b>	<b>54</b>
<b>8. MINIMUM-VARIANCE SYNTHETIC DISCRIMINANT FUNCTIONS</b>	<b>60</b>
<b>9. MODIFIED MSF SYNTHESIS BY FISHER AND MEAN-SQUARE ERROR TECHNIQUES</b>	<b>64</b>
<b>10. CORRELATION SYNTHETIC DISCRIMINANT FUNCTIONS</b>	<b>73</b>
<b>11. COMPUTER-GENERATED AND PHASE-ONLY SYNTHETIC DISCRIMINANT FILTERS</b>	<b>80</b>
<b>12. OPTICAL AI SYMBOLIC CORRELATORS: ARCHITECTURE AND FILTER CONSIDERATIONS</b>	<b>87</b>
<b>13. OPTICAL RELATIONAL-GRAPH RULE-BASED PROCESSOR FOR STRUCTURAL-ATTRIBUTE KNOWLEDGE BASES</b>	<b>94</b>
<b>14. MODEL-BASED SYSTEM FOR ON-LINE AFFINE IMAGE TRANSFORMATIONS</b>	<b>105</b>
<b>15. EVALUATION OF THE USE OF THE HOPFIELD NEURAL NET MODEL AS A NEAREST-NEIGHBOR ALGORITHM</b>	<b>114</b>
<b>16. NEAREST-NEIGHBOR NON-ITERATIVE ERROR CORRECTING OPTICAL ASSOCIATIVE MEMORY PROCESSOR</b>	<b>123</b>
<b>17. DISTORTION-INVARIANT ASSOCIATIVE MEMORIES AND PROCESSORS</b>	<b>142</b>
<b>18. PUBLICATIONS, PRESENTATIONS AND THESES PRODUCED</b>	<b>143</b>
18.1 PUBLICATIONS (AFOSR SUPPORTED, SEPTEMBER 1984-DATE)	143

18.1.1 PAPERS PUBLISHED UNDER AFOSR SUPPORT (September 1984- December 1985)	143
18.1.2 PAPERS PUBLISHED UNDER AFOSR SUPPORT DURING THE PRESENT TIME PERIOD (JANUARY-DECEMBER 1986)	146
18.1.3 PAPERS SUBMITTED UNDER AFOSR SUPPORT	148
18.1.4 BOOK EDITING AND BOOK CHAPTERS	150
18.2 PRESENTATIONS GIVEN ON AFOSR RESEARCH (AUGUST 1984-DATE)	150
18.3 THESES SUPPORTED BY AFOSR FUNDING (SEPTEMBER 1984-DATE)	155

## ABSTRACT AND SUMMARY

Our research concerns optical data processing for missile guidance and target recognition. It uses pattern recognition techniques with an increasing use of knowledge base, inference machine and associative processor techniques. Our Year 2 work addresses devices (the liquid crystal television), Kalman filters, intrinsic features, iconic filters, and symbolic processors. These all represent quite novel optical processing concepts. Our work also concerns new architectures and concepts such as: relational graph processors, optical linear discriminant processors, model-based optical processors, hierarchical symbolic optical correlators, and optical associative processors.



# 1. INTRODUCTION

The first year of this grant (1 October 1984 - 1 October 1985) produced much good work. This period was followed by an unsupported research period. By the end of our second year (January - December 1986) of this effort, we are again on track, having overcome various problems associated with no funding for one semester. Chapter 2 provides a summary overview of our calendar year 1986 research progress. Subsequent chapters detail each aspect of this research.

We are phasing out all feature extraction research and have now completed all student projects in this area. This work is summarized in Chapters 5 and 6. We have also ceased our Kalman filter research (since no Eglin Air Force Base funds were available to transition support of this work). Chapter 4 notes our final effort in this area. Our hierarchical symbolic processing concept is noted in Chapter 12. It utilizes correlation filters and thus we are continuing research in this area. This work is detailed in Chapters 7-11. After discussions with AFOSR, we have made a considerable redirection of our research effort toward optical computing rather than pattern recognition. Chapters 13-17 highlight five new research directions originated in 1986. These include: relational graph processors, model-based processors, and analysis of the Hopfield associative memory, new nearest neighbor data matrix associative processors, and distortion-invariant associative processors. These represent four new optical approaches to advanced computing.

In 1986, the Principal Investigator (PI) was quite active with various invited papers on numerous topics: the IEEE Spectrum article (August 1986), an SPIE Institute Series paper on scene analysis [5], an Optics News special issue article [7]. He also has been most active in various conference organizations. He was Chairman of a hybrid image processing conference (April 1986), Chairman of a digital image processing session (January 1986), Chairman of a set

of six conference on robotics (October 1986), plus provided an invited paper at the ICALEO'86 conference. We have thus expended considerable effort to expose our work and AFOSR research to a quite wide community.

## **2. SUMMARY AND OVERVIEW**

We now provide a summary and overview of our 1986 research progress and highlight the contents of Chapters 3-17 which detail 15 different aspects of our research.

### **2.1 SPATIAL LIGHT MODULATORS (SLMs) (Chapter 3, Liquid Crystal Television Correction)**

SLMs represent the critical element in most optical processors. The liquid crystal television (LCTV) emerged in late 1985 as a low-cost and viable optical SLM. Our work [8] on this device included practical remarks about bias voltage selection and polarization reorientation, the demonstration of interpolation on the device by single sideband filtering, and the selection of beam balance ratio spatial filtering techniques using such a sampled input SLM. Our primary contribution was the use of a new phase conjugate hologram correction technique to correct for the phase nonuniformity of the device. This allows its use in a space integrating correlator, as we experimentally demonstrated.

### **2.2 FACTORIZED KALMAN FILTER (KF) ALGORITHM (Chapter 4)**

This chapter concludes our AFOSR work in this area [15]. ONR/SDI support for this may allow us to continue some of this work. This 1986 work involves a new parallel vectorized and factorized KF algorithm. This is very suitable for optical processing, since it requires a reduced accuracy optical processor. This is achieved since the algorithm does not entail processing full matrices, nor does it involve square root and other time-consuming operations. We have detailed how this algorithm can be employed on an optical processor.

## 2.3 FEATURE EXTRACTION (MOMENTS, FOURIER TRANSFORMS AND HARTLEY TRANSFORMS) (Chapters 5 and 6)

This work concludes our intrinsic (or feature extraction) OPR (optical pattern recognition) research. We feel that optics has a considerable role in low-level vision, where the input data rate is the highest and where the number of operations per input data pixel or point is the largest. One thrust of this research has been to provide more features from one optical feature space. This is attractive since separate optical architectures are then not necessary for each desired feature space. Chapter 5 considers an optical Fourier transform feature space (this is the simplest feature space that one can optically generate). We show in this chapter how the moments can be obtained from this feature space [16]. We also provide a new digital filtering technique and algorithm to aid calculation of moments from Fourier coefficients [17]. Chapter 5 summarizes this work [18] and conference paper [19] provides new simulation results on detector area effects and other results using this feature space.

The basic architecture involves an optical Fourier transform system with and without a linear  $x$  mask present. The Fourier transform produced by this system is sampled, and an approximate derivative is digitally produced by a differentiating finite impulse response filter using a new algorithm and techniques. The associated moments are then assembled from these samples. Techniques to achieve this with and without a linear  $x$  mask are noted. In total, 21 samples of the Fourier transform are used to produce 21 moments. For the case of symmetric inputs, we find the odd order moments above third order are in error by over 7%. For asymmetric inputs (these are typical of most real objects), all moments up to eighth-order are accurate within 2%. We found that the sampling of this system was optimal at  $1/4L$  (where  $L$  is the size of the input). We also found that as the digital filter length increases, the number of usable moments also increases (with a filter length of 15 being adequate for all moments up to

order 5). Detector area effects were also considered (such as area sampling, which was found to be a small negligible error compared to the filter length effect). Concerning detector dynamic range, we found that a 16-bit A/D converter was adequate. Our noise analysis showed that approximately 0 dB input plane SNR could be tolerated. Our initial results showed very good separation of different tool parts for different rotated and translated versions of these input images.

We also provided a journal paper [4] in 1986 that detailed the computer generated hologram fabrication of a wedge ring detector with experimental data on this system included.

We have also [24] detailed how one can obtain the Hartley transform from the Fourier transform and how one can obtain moments from the Hartley transform (Chapter 6). This implementation technique is quite attractive since no additional mask is now required. This arises because the Hartley transform is real. The Hartley transform has other attractive properties as well. These are discussed in the aforementioned reference. We have also developed a new algorithm to recursively calculate all moments from the n-derivatives of the Hartley transform at the origin. This thus represents additional work associated with producing various feature spaces from and on the same optical processor.

Paper [25] discusses other uses for this system and proves that all geometrical moments can be calculated recursively from the partial derivatives near the origin in the Hartley transform intensity pattern.

## **2.4 APPROACHES TO LARGE-CLASS ANALYSIS PROBLEMS**

### **(Chapters 7 and 12)**

As noted in Chapter 1, our approach we consider for advanced processors involves a hierarchical symbolic correlator. The basic concepts of such a processor [21] are advanced in

Chapter 12. They involve the use of multiple hierarchical levels of different advanced distortion-invariant filters. This yields a unique symbolic processor, whose outputs are the spatial representation of the input data for different correlation filters.

In 1986, various aspects of iconic filters were studied and several new concepts emerged. Chapters 7-10 detail these results. In Chapter 7, we analyze the simplest filter (an equal correlation peak (ECP) filter) assuming Gaussian and exponential image models for the correlation functions [22] with attention to the large-class problems. Various effects (space bandwidth product, in-plane scale and rotation distortion, noise, and the number of training images) are investigated in terms of the output SNR for an ECP projection synthetic discriminant function (SDF). Quantitative data on all issues are advanced. Similar results are obtained for both image models. This is encouraging, since the results should thus be extendible to more general models and to real imagery. We also find that as the number of training images increases, the best SNR decreases and the worst-SNR increases. We also find larger differences between the best and worst-case SNR as the space bandwidth product increases. These results provide us with many useful guidelines:

1. increases in the training set size (beyond some value  $N$ ) will cause little improvement,
2. more training set images are useful for larger space bandwidth product images,
3. smaller space bandwidth product images may yield higher SNR outputs when the number of training images  $N$  is limited.
4. for each  $N$  selected, there is an optimum space bandwidth product.

We plan to employ these results in our future hierarchical symbolic processor research.

Our 1000 class OCR (optical character recognition) results [14] represent the first case study data on a large class optical processor. The first multi-level and multi-filter optical processor studies are included in this work. Also included are the first attention to the effects of a large number of object classes (as occurs in the advanced inference and optical computing and

AI (artificial intelligence) processors using knowledge bases, that we consider). These results should be most attractive and appropriate for advanced optical AI, symbolic, and optical computing architectures.

## 2.5 NEW ICONIC FILTERS FOR HIERARCHICAL PROCESSORS (Chapter 8-10)

Chapter 8 details our minimum variance SDF iconic filter [23]. This theoretical study advances the case of a linear combination filter and when such a filter is best, and the performance of the conventional SDF in the presence of colored (real) noise (versus its performance in white Gaussian noise). It also advances cases of a nonlinear discriminant function. We constrain the integrated intensity of the filter in all images to be unity (rather than assuming a linear combination filter). For the case of white noise, we found that the filter that minimizes the output noise variance is the linear combination ECP projection SDF that we previously developed. In colored noise, the optimal filter is a different linear combination filter function. The inverse of the covariance matrix  $C$  of the noise is required to obtain this optimal SDF. This covariance matrix inverse is not always easily obtained. Approximations to it are one of various future research topics possible. The suboptimality of the conventional ECP-SDF in colored noise is also quantified in this chapter.

We also devised [1] new Fisher and mean square error (MSE) filter functions (Chapter 9). These filters use a reduced orthogonal basis function set and conventional pattern recognition synthesis techniques. They are fabricated such that conventional parameters for pattern recognition are optimized. This is attractive from a theoretical standpoint. These filters also offer promise for fabricating reduced dynamic range and special (i.e. binary and phase only) filter functions.

As noted at the outset, these various filter functions are planned to play a significant role

in our advanced hierarchical correlator and iconic filter as well as symbolic processor architectures and algorithms (Chapter 12).

New correlation filters and peak to sidelobe ratio (PSR) filters (Chapter 10) that are superior to the original projection SDF filters were also detailed [11]. The projection filters constrain only the peak value of the correlation function. The correlation filters control the shape of the correlation function and the PSR filters provide easily detectable correlation peaks. These three filters are employed in our hierarchical correlator architecture and concept [3,22].

## **2.6 COMPUTER GENERATED HOLOGRAM (CGH) FILTER SYNTHESIS (Chapter 11)**

This task study concerns the number of amplitude and phase levels required in a correlation filter [20]. Large class problems are considered. We find that phase-only filters are inferior for discrimination and in large class cases. Several amplitude levels are found to significantly improve performance.

## **2.7 OPTICAL ARTIFICIAL INTELLIGENCE (Chapters 13-17)**

These chapters advance four new concepts for advanced optical computing. This work involves a relational graph processor [2,12]. This also includes the concept of an optical linear discriminant function, techniques to organize a knowledge base, and the concept of a parallel data base search (Chapter 13). Our work has also advanced the first optical use of a model-based representation [6] (Chapter 14) for input objects. Advances in graphics can be expected to make this approach most attractive, especially for advanced large data base cases. It is very attractive in terms of computer memory requirements, filter generation for correlators and for associative processor memory systems as detailed elsewhere (Chapter 12). We conducted detailed initial studies [26] that noted severe storage problems with the Hopfield associative memories and that the nature of the input data to such processors was quite restrictive and was



thus not the general vectors required for pattern recognition (Chapter 15). We then advanced a data matrix nearest neighbor associative processor [27] that is preferable (Chapter 16). Our final contribution [13] has involved distortion-invariant associative processors (Chapter 17). This work includes the first quantitative data on such processors, new synthesis techniques for these processors and new synthesis techniques to improve their memory capacity. One general paper on this work [9] was published in 1986. Attention to optical processing techniques for range image data were also advanced [10]. Several invited papers at the January 1987 SPIE conference on this area will be available shortly.

## CHAPTER 2 REFERENCES

1. D. Casasent and W. Rozzi, "Modified MSF Synthesis by Fisher and Mean-Square Error Techniques", *Applied Optics*, Vol. 25, pp. 184-187, 15 January 1986.
2. D. Casasent and A.J. Lee, "A Feature Space Rule-Based Optical Relational Graph Processor", *Proc. SPIE*, Vol. 625, pp. 234-243, January 1986.
3. D. Casasent, "Optical AI Symbolic Correlators: Architecture and Filter Considerations", *Proc. SPIE*, Vol. 625, pp. 220-225, January 1986.
4. D. Casasent, S.F. Xia, J.Z. Song, and A.J. Lee, "Diffraction Pattern Sampling Using a Computer-Generated Hologram", *Applied Optics*, Vol. 25, pp. 983-989, 15 March 1986.
5. D. Casasent, "Scene Analysis Research: Optical Pattern Recognition and Artificial Intelligence", *SPIE, Advanced Institute Series on Hybrid and Optical Computers*, Vol. 634, Leesburg, Virginia, March 1986.
6. D. Casasent and S.A. Liebowitz, "Model-Based System for On-Line Affine Image Transformations", *Proc. SPIE*, Vol. 638, pp. 66-75, March-April 1986.
7. D. Casasent, "Optical Computing at Carnegie-Mellon University", *Optics News, Special Issue on Optical Computing*, Vol. 12, pp. 11-13, April 1986.
8. D. Casasent and S.F. Xia, "Phase Correction of Light Modulators", *Optics Letters*, Vol. 11, pp. 398-400, June 1986.
9. D. Casasent, "Optical Artificial Intelligence Processors", *IOCC-1986 International Optical Computing Conference, Proc. SPIE*, Vol. 700, July 1986, pp. 246-250, 1986.
10. S.A. Liebowitz and D. Casasent, "Hierarchical Processor and Matched Filters for Range Image Processing", *Proc. SPIE*, Vol. 727, October 1986.
11. D. Casasent and W.T. Chang, "Correlation Synthetic Discriminant Functions", *Applied Optics*, Vol. 25, pp. 2343-2350, 15 July 1986.
12. D. Casasent and A.J. Lee, "Optical Relational-Graph Rule-Based Processor for Structural-Attribute Knowledge Bases", *Applied Optics*, Vol. 15, pp. 3065-3070, 15 September 1986.
13. D. Casasent and B. Telfer, "Distortion-Invariant Associative Memories and Processors", *Proc. SPIE*, Vol. 697, August 1986.
14. A. Mahalanobis and D. Casasent, "Large Class Iconic Pattern Recognition: An OCR Case Study", *Proc. SPIE*, Vol. 726, October 1986.

15. J. Fisher, D. Casasent and C.P. Neuman, "Factorized Extended Kalman Filter for Optical Processing", *Applied Optics*, Vol. 25, pp. 1615-1621, 15 May 1986.
16. B.V.K. Vijaya Kumar and C. Rahenkamp, "Calculation of geometric moments using Fourier plane intensities", *Applied Optics*, Vol. 25, pp. 997-1007, 1986.
17. C. Rahenkamp and B.V.K. Vijaya Kumar, "Modifications to the McClellan, Parks and Rabiner computer program for designing higher order differentiating FIR filters", *IEEE Trans. ASSP*, Vol. 34, pp. 1671-74, December 1986.
18. B.V.K. Vijaya Kumar and C. Rahenkamp, "An optical/digital hybrid system for calculating geometric moments", *SPIE Proc.*, Vol. 579, pp. 215-224, 1985.
19. B.V.K. Vijaya Kumar and C. Rahenkamp, "Performance of a hybrid processor to compute geometric moments", *SPIE Proc.*, Vol. 638, pp. 32-40, March-April 1986.
20. D. Casasent and W. Rozzi, "Computer-Generated and Phase-Only Synthetic Discriminant Function Filters", *Applied Optics*, Vol. 25, pp. 3767-3772, 15 October 1986.
21. D. Casasent, "Optical AI Symbolic Correlators: Architecture and Filter Considerations", *Proc. SPIE*, Vol. 625, pp. 220-225, January 1986.
22. B.V.K. Vijaya Kumar and E. Pochapsky, "Signal-to-noise ratio considerations in modified matched spatial filters", *JOSA-A*, Vol. 3, pp. 777-786, June 1986.
23. B.V.K. Vijaya Kumar, "Minimum variance synthetic discriminant functions", *JOSA-A*, Vol. 3, pp. 1579-84, October 1986.
24. B.V.K. Vijaya Kumar, "Geometric moments computed from the Hartley transform", *Optical Engineering*, Vol. 25, pp. 1327-32, December 1986.
25. B.V.K. Vijaya Kumar, "Geometric moments from Hartley transform intensities", *SPIE Proc.*, Vol. 639, pp. 253-59, March-April 1986.
26. B. Montgomery and B.V.K. Vijaya Kumar, "Evaluation of the use of the Hopfield neural net model as a nearest-neighbor algorithm", *Applied Optics*, Vol. 25, pp. 3759-66, 15 October 1986.
27. B. Montgomery and B.V.K. Vijaya Kumar, "Nearest-neighbor non-iterative error correcting optical associative memory processor", *SPIE Proc.*, Vol. 638, pp. 83-90, March-April 1986.

**3. PHASE CORRECTION OF LIGHT**  
**MODULATORS**

## Phase correction of light modulators

David Casasent and Shao-Feng Xia\*

Carnegie-Mellon University, Department of Electrical and Computer Engineering, Pittsburgh, Pennsylvania 15213

Received February 18, 1986; accepted March 31, 1986

A new and inexpensive holographic technique for measuring the phase errors of a two-dimensional spatial light modulator (SLM) is described, and experimental verification is provided. A new technique to correct spatial phase errors in any SLM is then detailed and experimentally demonstrated. This technique is employed for the Radio Shack liquid-crystal television SLM, and a shift-invariant correlator is obtained. Additional low-pass filtering techniques (appropriate for any SLM with a fixed pattern of modulating cells) are discussed that provide improved contrast and achieve proper correlations.

Liquid-crystal displays<sup>1</sup> represent inexpensive spatial light modulators (SLM's) that are readily available and should make real-time optical computing accessible to more researchers. The Radio Shack liquid crystal (LC) TV has received the majority of recent attention.<sup>2,3</sup> Its major shortcomings are its low contrast and poor optical quality. In this Letter we offer methods to improve the contrast of the device and to compensate for the spatial phase variations of this device. The lack of optical flatness of the device prevents its use in most coherent optical processing applications. Specifically, without shift invariance it cannot be used in a correlator. Recently the use of this device in a liquid gate with mineral oil was reported, and this was found to remove phase variations of the device.<sup>3</sup> The need for high-quality 7.5-cm diameter or larger optical flats and packaging plus sealing problems will significantly increase the cost of a system that uses this phase-correction technique. Also, many SLM's cannot be immersed in the index-matching material of a liquid gate. The technique that we advance is less expensive and of more general use for phase correction of such light modulators. We emphasize the use of the Radio Shack LC but note that the technique described is of general use for many other SLM's.

By way of review and for completeness, we summarize the LC properties of interest in this Letter. The device is 5.4 cm × 5.4 cm in size with 146 × 120 elements each 370 μm × 370 μm. The brightness control affects the bias voltage on each cell, and the video or computer input signals to the device provide variations or modulations about the operating point chosen by the brightness (bias) control. For linear operation and high dynamic range, the device is best operated from -0.3 to -0.5 V, with a bias of -0.4 V. A maximum transmittance of approximately 50% then results. When the bias is much lower, at -1.2 V, the off level of the device has been noted<sup>2</sup> to be much less, but the maximum transmittance is only 5% in this case (owing to limitations on the video voltage levels obtainable with present units). The tilt and twist of the LC molecules vary with the applied voltage, and this affects the polarization of the output light. Thus we note that when the minimum (or maximum) applied

voltage is known, one can properly rotate the polarizers between which the LC is sandwiched to obtain the best off (or on) state transmittance. The polarizers on the unit are not necessarily optimally aligned with the LC molecules, and the polarizers provided with the unit have a worse optical flatness than the LC itself and thus generally should be replaced. Thus polarization alignment is necessary in all units for best performance. In the interferometric experiments noted in this Letter, care was taken to choose the best polarization for the data leaving the LC device and for the reference beams. This significantly improves performance by optimizing the contrast of the interference patterns provided.

The contrast (the ratio of the maximum to minimum transmittance) of the device has been noted to be 25:1. However, under dynamic operation and with the practical case of a fixed bias, the contrast is much less (typically 2:1 or 4:1). Attention must be given to the method by which this contrast ratio is measured, as we now discuss. Because of the regular grid structure of the cells in the device, the Fourier-transform (FT) pattern of any input data has many orders (horizontal and vertical) spaced at intervals proportional to the reciprocal of the cell spacing (370 μm). If the contrast of the device is measured in the output plane of a two-lens imaging system, then all orders contribute to the output image; thus the background level is considerably increased, and the measured contrast ratio decreases. However, when only the zero-order pattern in the FT plane is passed, the output background level is significantly reduced. The cross-sectional scan of the image of a vertical bar is shown in Fig. 1(a). The output image with only the zero order in the FT plane passed is shown in Fig. 1(b). The contrast ratio can be increased to 10:1 by this technique. When the LC is used as the input plane SLM of a correlator, care must be taken not to include the FT of the regular grid structure on the matched spatial filter (MSF). If this is done, the correlation will be based on the regular LC cell structure as well as on the information recorded on the unit. One can reduce the effect of the regular grid structure of this device by emphasizing the proper spatial frequencies during

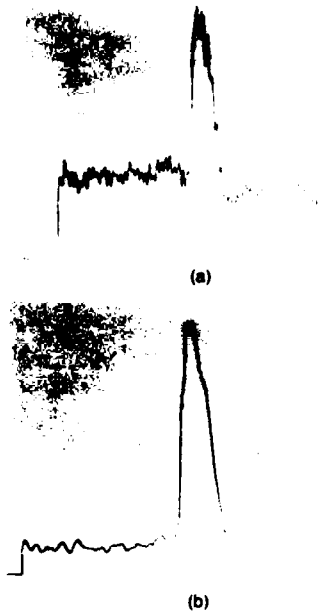


Fig. 1. Output image of a vertical bar on the LC TV with a two-lens imaging system: (a) with no filter present; (b) with only the zero order passed.

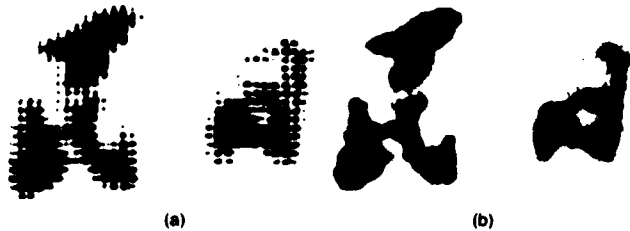


Fig. 2. Output image of Chinese characters: (a) with no filter present; (b) with only the zero order passed.

MSF synthesis. However, passing only the zero-order version of the input image is much preferable. Figure 2(a) shows the image of two Chinese characters on the LC TV, and Fig. 2(b) shows the output image with only the zero order passed. As seen, the regular LC pattern is quite significant in the order image data and is removed (and thus does not contribute to the output correlation) by the zero-order filtering noted. The pattern now appears continuous rather than sampled, because of the sinc function interpolation provided by the FT plane square aperture used (which passes only the zero-ordered data).

Next we consider the optical flatness of the LC TV. Quantitative measurements of this have yet to be provided in the literature. One can obtain these data by a classic Michelson interferometer system. However, such a system requires mirrors and beam splitters of large 7.5-cm diagonal size. Such components are available, but we have devised a new technique (Fig. 3) to achieve quantitative optical flatness phase information on SLM's at a significantly reduced cost. With the LC TV (sample) removed from the system, we form the holographic interference pattern of the signal and reference beam on a Kodak 649F plate at  $P_2$ .

This plate was developed, bleached, and repositioned at  $P_2$ . When the plate is reilluminated with the reference beam only, the original signal beam is reconstructed traveling to the right in the original direction and with no phase distortions present on it. If the LC TV is now placed at plane  $P_1$  and illuminated from the left, a new signal beam (with phase variations proportional to the optical flatness variations of a LC device) travels through  $P_2$  to  $P_3$ . The interference of the original signal beam (produced by the reference beam and the hologram plate) and the signal beam passing through the LC TV is formed at the observation plane  $P_3$ . The  $P_3$  pattern without the sample present is shown in Fig. 4(a) and demonstrates the high quality of the measurement system. The  $P_3$  pattern with the LC TV at  $P_1$  present during reconstruction is shown in Fig. 4(b). From a detailed analysis of the interferogram, we find local optical flatness variations to be  $3\lambda$  and the worst-case variations to be  $10\lambda$ . The original polarizers on the LC TV are quite poor, as Fig. 4(c) shows.

To correct for these phase variations and to provide a shift-invariant correlator by using the LC TV as the input SLM, we formed a phase-conjugate correction hologram. Figure 5(a) shows the hologram synthesis system. Denoting the phase distortions of the LC and the polarizers by  $\phi_1(x, y)$  and  $\phi_2(x, y)$ , the amplitude distribution of the light passing through the LC device

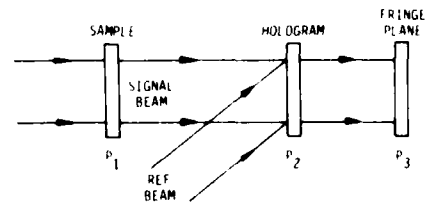


Fig. 3. Holographic phase-distortion measurement system.

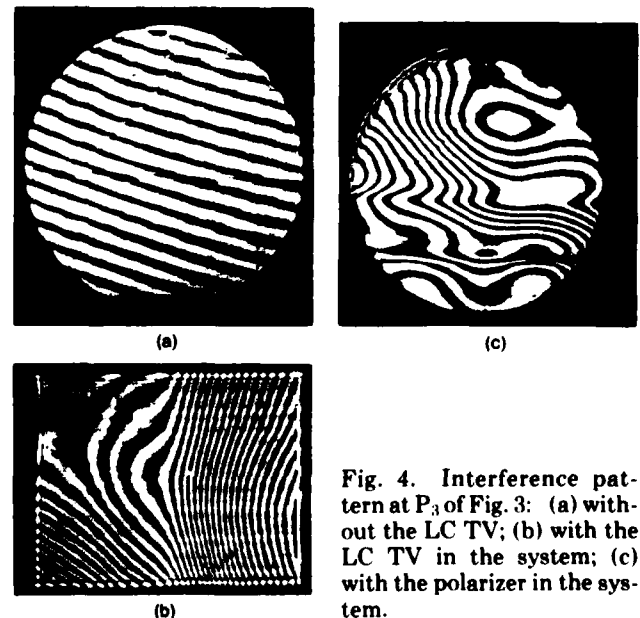


Fig. 4. Interference pattern at  $P_3$  of Fig. 3: (a) without the LC TV; (b) with the LC TV in the system; (c) with the polarizer in the system.

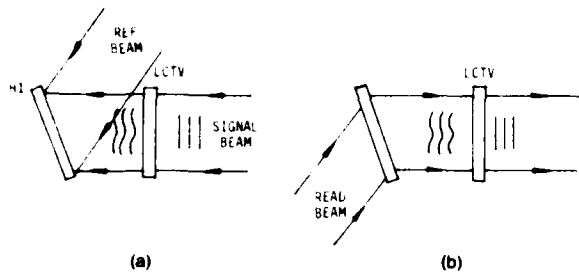


Fig. 5. Optical system for (a) synthesis and (b) use of the phase-conjugate hologram H1 to correct LC TV distortions.

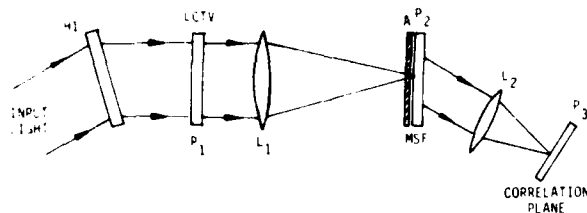


Fig. 6. Optical frequency plane correlator using the LC TV and the phase-conjugate hologram H1.

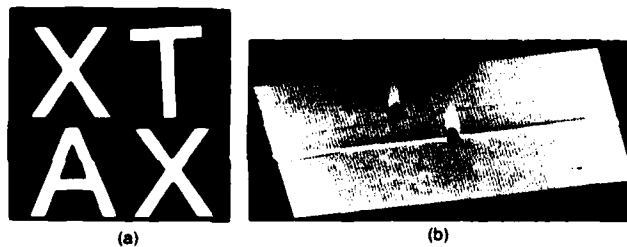


Fig. 7. (a) Input image to the LC TV. (b) The  $P_3$  correlation plane pattern with a MSF of the letter X placed at  $P_2$ .

(with no applied electrical signal) is  $g(x, y) = \exp[j(\phi_1(x, y) + \phi_2(x, y))]$ . The interference of  $g(x, y)$  and a plane-wave reference beam is formed on a glass plate H1. This plate is then developed, bleached, and repositioned in the original location in the system. When illuminated with the conjugate of the reference beam as shown in Fig. 5(b), the light distribution leaving H1 is proportional to  $g^*(x, y)$ . If the image infor-

mation on the LC TV is described by  $f(x, y)$ , then the light distribution leaving the LC and the polarizer system is  $g^*(x, y)f(x, y)g(x, y) = f(x, y)$ , i.e., the image information only with all phase and thickness variations of the SLM canceled by the phase-conjugate hologram H1. Bleaching of H1 results in negligible light loss in this correction system. In all laboratory experiments, the polarizers are oriented for the optimum contrast, and the polarization of the reference beam is made parallel to that of the signal beam to optimize interference.

The optical correlator of Fig. 6 was assembled and used to test the shift invariance of our phase-conjugate hologram H1 and the LC TV system. The FT of the input at  $P_1$  is formed at  $P_2$ , the zero order only is passed by the aperture A, a MSF is placed at  $P_2$ , and the correlation appears at  $P_3$  (where it is detected and observed on an isometric display). The LC TV input at  $P_1$  is real-time from a camera. In Fig. 7(a) we show a  $P_1$  input pattern with two occurrences of the letter X. An MSF of the letter X was formed and placed at  $P_2$ . An isometric display of the  $P_3$  correlation plane is shown in Fig. 7(b). Both peaks are approximately equal in strength, and the shift invariance of the phase-conjugate correction technique has been demonstrated. Without the H1 correction plate, only one correlation peak could be detected, and it was quite weak in strength. The simple technique shown in Fig. 6 of illuminating the input to an optical correlator through the phase-conjugate hologram H1 appears to be appropriate for permitting the use of many inexpensive devices in real-time coherent optical computing.

The research reported on herein was supported by the U.S. Air Force Office of Scientific Research and General Dynamics-Pomona Internal Research and Development Funds.

\* Permanent address, Fudan University, Fudan, China.

## References

1. S. Morozumi, K. Oguchi, and H. Ohshima, *Opt. Eng.* **23**, 241 (1984).
2. H. K. Liu, J. Davis, and R. Lilly, *Opt. Lett.* **10**, 635 (1985).
3. J. Davis, R. A. Lilly, K. D. Krenz, and H. K. Liu, *Proc. Soc. Photo-Opt. Instrum. Eng.* **613** (to be published, 1986).

**4. FACTORIZED EXTENDED KALMAN FILTER**  
**FOR OPTICAL PROCESSING**



END

7-87

DTIC